Optical Arbitrary Waveform Generation (OAWG) Based on RF Injection-Locked Kerr Soliton Combs

D. Fang(1,5), H. Peng(1,5), D. Drayss(1), Y. Chen(1), C. Füllner(1), A. Sherifaj(1), G. Lihachev(3), W. Freude(1), S. Randel(1), T. J. Kippenberg(3), T. Zwick(2), C. Koos(1)

(1) Inst. of Photonics and Quantum Electr. (IPQ) / Inst. of Microstructure Techn. (IMT), Karlsruhe Institute of Technology (KIT), Germany; (3) Inst. of Radio Frequ. Engineering and Electronics (IHE), Karlsruhe Institute of Technology (KIT), Germany; (4) Swiss Federal Institute of Technology Lausanne (EPFL), Lausanne, Switzerland; (5) Contributed equally; dengyang.fang@kit.edu, huanfa.peng@kit.edu, christian.koos@kit.edu

Abstract *We demonstrate the first optical arbitrary-waveform generator that relies on a Kerr-soliton microcomb as a multi-wavelength light source. The concept combines RF injection-locking of the comb-tone spacing with phase-stabilized spectral stitching. We demonstrate high-quality 288 GBd 64QAM transmission along with spread-spectrum communications at SNR down to −17 dB. © 2023 The Author(s)*

Introduction

Comb-based optical arbitrary waveform generation (OAWG) can overcome the bandwidth limitations of electronic waveform generation by efficient multiplexing of spectrally-sliced tributary signals in the optical domain [1-3]. On a technical level, these schemes crucially rely on comb sources that provide phase-locked carriers and that can be synchronized to the electronic signal generators used to generate the tributaries. The most straightforward way of generating combs with electronically controlled line spacings and inter-line phase relations is to use continuous-wave (CW) lasers in combination with electrically driven modulators [4]. However, while this concept has been the mainstay for OAWG demonstrations so far [1-3], the number of tones obtained from modulator-based combs is limited, hence restricting the bandwidth scalability of the overall scheme. Moreover, cascaded modulator arrangements are often bulky and power-hungry. In contrast to that, chip-scale Kerr soliton microcombs are compact and can offer broadband spectra with hundreds of lines [5]. However, all microcombs so far used in signal-processing experiments have been free-running, without any possibility to control the comb-line spacing or the associated phase relations. While this problem can be overcome by dedicated digital signal processing (DSP) schemes for optical arbitrary waveform measurement (OAWM) [6,7] or comb-based ranging [8], it has so far prevented the use of Kerr combs in OAWG schemes.

In this paper, we show that these limitations of Kerr soliton microcombs can be overcome by radio-frequency (RF) injection locking. In this approach, a phase-modulated pump is used to seed the Kerr-generated comb tones in the resonance next to the pumped one, thus synchronizing the line spacing and the inter-line phase relation of the entire comb to a highly stable radio frequency (RF) oscillator. This approach allows to synchronize the RF injection-locked comb source with a spectrally-sliced OAWG system that is based on a recently reported feedback-controlled phase stabilization scheme [2,3], thereby allowing generation of seamlessly stitched signal spectra with well-defined overall phase relations and precisely defined time-domain waveforms. To the best of our knowledge, our experiments represent the first demonstration of an OAWG based on a Kerr microcomb as a multi-wavelength light source. In a proof-of-concept experiment, we use an RF injection-locked Kerr microcomb with a line spacing of f_{FSR} = 35.66125 GHz to demonstrate four-slice OAWG with carrier spacing of $2f_{FSR}$ = 71.32250 GHz, leading to an overall bandwidth of approximately 295 GHz. To demonstrate the viability of the scheme, we combine it with a spectrally-sliced OAWM system [9] and perform different signaling and transmission experiments. In a first set of experiments, we generate 64QAM at symbol rates of up to 288 GBd, which are finally transmitted over 87 km of standard single-mode fiber (SMF). To the best of our knowledge, this is the highest symbol rate so far demonstrated for 64QAM. In a second set of experiments, we demonstrate spread-spectrum communications by spreading 2 GBd signals with various modulation formats up to 128QAM over an optical bandwidth of 288 GHz and by transmitting them over 87 km SMF at a negative signal-to-noise ratio (SNR) down to −17 dB. We show that we can still reconstruct the information using our OAWM system with a bit error ratio (BER) below the threshold for soft-decision forward error correction (SD-FEC) with 20% overhead. To the best of our knowledge, this is the first demonstration of OAWG-based spread-spectrum optical transmission. We believe that our work is an important step towards ultra-broadband OAWG schemes that leverage chip-scale Kerr frequency combs as highly scalable multi-wavelength light sources, thus paving a path towards waveform generation at THz bandwidths.

Concept and implementation

Figure 1(a) shows the concept and setup of our spectrally-sliced OAWG system, comprising an RF injection-locked Kerr comb generator that relies on a fiber-packaged Si_3N_4 ring resonator with a Q-factor of approximately 6.5 million. The fabrication of the Si_3N_4 ring resonators relies on the photonic Damascene process [10], and the fiber-chip connections in the comb-generator package are based on photonic wire bonds (PWB) [11], see Fig. 1(b). The measured total coupling loss is approximately 2 dB per PWB interface. We use a continuous-wave tone from an external-cavity laser (ECL) to pump the comb source. To synchronize the comb line spacing to an RF oscillator, the pump is first modulated using a phase modulator (PM), which is driven by an RF oscillator (RF osc.) with a frequency close to the line spacing (free spectral range, FSR) of the free-running comb. This leads to an additional sideband in the optical spectrum of the pump, which falls into a ring resonance adjacent to the pumped one and which acts as a seed for the Kerr-generated comb tone associated with this resonance. The Kerr soliton comb can thus be synchronized with the RF oscillator drive signal provided that the frequency difference between the modulator-generated seed tone and the position of the “native” comb line, that would emerge in absence of pump modulation, is within the locking range [12]. The optical spectrum of the generated comb locked to a 35.66125 GHz oscillator at Point Ⓐ is shown in Fig. 1(c). For our OAWG experiment, we select four tones from the region marked with an orange dotted line using a wavelength-selective switch (WSS), see Fig.1(d). Note that the WSS only selects every second line, such that the

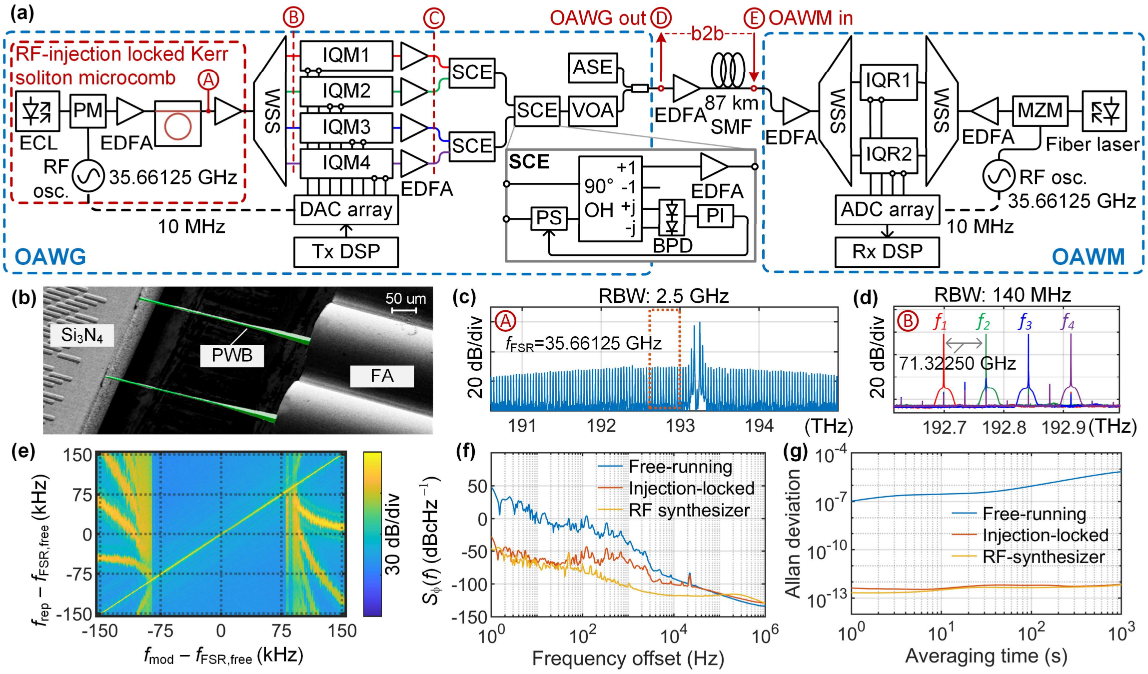

Fig. 1: Concept and setup of the experiment for an optical arbitrary waveform generator (OAWG) with an RF injection-locked Kerr comb, combined with a spectrally-sliced optical arbitrary waveform measurement (OAWM) system. **(a) OAWG:** The pump for the Kerr microring is generated by modulating a continuous-wave external-cavity laser (ECL) with a phase modulator (PM), driven by an RF synthesizer at a frequency close to the free-running FSR of the comb of approximately $f_{\mathrm{FSR,free}}$ = 35.66125 GHz. Four comb lines spaced by twice the FSR are selected by a wavelength-selective switch (WSS) and serve as phase-locked carriers for generation of the tributary signals in four IQ-modulators (IQM1…4), which are driven by a DAC array synchronized to the Kerr comb repetition rate using a 10 MHz clock. The four tributary signals are coherently combined using phase-stabilized signal combing elements (SCE) to form the target waveform. Each SCE consists of a phase controller and a 90° optical hybrid (OH), which is fed with adjacent overlapping slices. A balanced photodetector (BPD) at the quadrature outputs is used to detect the phase errors, and a PI circuit provides the drive signal for a phase shifter (PS) that minimizes the phase error. A variable optical attenuator (VOA) can be combined with an amplified spontaneous emission (ASE) noise source for sweeping the signal-to-noise ratio (SNR) of the generated waveform. **OAWM:** A WSS decomposes the generated broadband signal into two slices, which are then routed to two IQ receivers (IQR1…2). Two phase-correlated tones from a comb generated by a Mach-Zehnder modulator (MZM) are selected by another WSS as serve as LO tones for the IQR. The IQR outputs are connect to an ADC array followed by digital signal processing (Rx DSP) for signal reconstruction [ref9]. **(b)** Fiber-packaged integrated Si_3N_4 microring connected to fiber arrays (FA) via photonic wire bonds (PWB). **(c)** Optical spectrum of RF injection-locked Kerr soliton comb at Point Ⓐ; region of the selected comb lines indicated by orange dotted lines. **(d)** Selected amplified phase-locked tones spaced by $2f_{\mathrm{FSR}}$ =71.32250 GHz at Point Ⓑ. **(e)** Spectrogram showing the injection locking range of approx. ±75 kHz. **(f)** RF phase noise of the Kerr soliton comb in free-running and injection-locked state, compared to that of the RF synthesizer. **(g)** Measured Allan deviation of the RF synthesizer frequency and of the comb repetition rate before and after injection-locking.

spacing of the selected comb lines amounts to $2f_{\mathrm{FSR}}$ = 71.32250 GHz. These comb lines are then individually modulated by four IQ modulators (IQM), which are driven by eight digital-to-analogue converter (DAC) channels synchronized to the RF oscillator via a10 MHz clock. The spectra of the four resulting tributary signals overlap slightly and are merged by a binary tree of three signal-combining elements (SCE). For stabilizing the phases with which the tributary signals are stitched, each SCE comprises a phase shifter (PS) at one input port, and a subsequent 90° optical hybrid (90° OH) that combines the signals at the positive port of the in-phase output (+1), while the two quadrature output ports (+j, -j) are routed to a low-speed balanced photodetector (BPD). This BPD detects the phase-error signal generated by interference of overlapping spectral components from adjacent spectral slices, see [2] for details. The error signal is continuously monitored, and a proportional-integral (PI) controller implemented on an FPGA board generates the corresponding drive signal for the phase shifter to minimize the error signal. This leads to the stable generation of the envisaged waveform. Note that the phase shifter in our current implementation has only a finite range such that resets are needed every now and then. This can be avoided by using endless phase shifters [13].

To analyze the generated broadband signal, we exploit a spectrally-sliced OAWM receiver similar to the one in [9]. The received optical waveform is first decomposed into two tributary signals by a WSS, which are then coherently detected by a pair of IQ receivers (IQR1…2). The associated LO tones are derived from a modulator-generated frequency comb and separated by a second WSS. The spacing of the two tones is 142.645 GHz, which allows our OAWM system to cover a detection bandwidth of more than 300 GHz by using 80 GHz analogue-to-digital convertors (ADC) at the outputs of the IQR. Details about the calibration of the OAWM and the associated signal reconstruction can be found in [9].

To investigate the performance of the RF injection locking of the Kerr comb at the OAWG, we first generate a comb with a free-running FSR of approximately $f_{\mathrm{FSR,free}}$ = 35.66125 GHz, and then apply a frequency-swept (f_{mod}) phase modulation to the pump while monitoring the RF spectrum, generated by direct detection of the comb on a high-speed photodiode. The resulting spectrogram around the RF beat tone is shown in Fig. 1(e). Synchronization of the comb FSR (f_{rep}) and the RF modulation occurs when the frequency difference between them is below 75 kHz, corresponding to a locking range of approx. 150 kHz. Figure 1(f) shows the single-sideband (SSB) phase noise spectrum $S_\phi(f)$ of the RF tone at the comb FSR frequency, generated in the free-running (blue) and the injection-locked state (orange), along with the phase noise of the RF modulation signal (yellow). For offset frequencies below 100

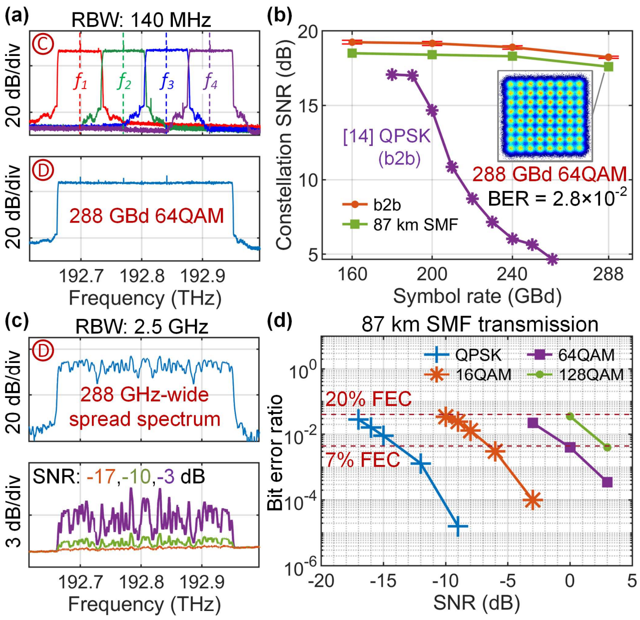

Fig. 2: Functional demonstration. **(a) Top:** Sliced spectra of tributaries generated by IQM1…4, measured at Point Ⓒ in Fig. 1(a); **Bottom**: Coherently combined tributaries at Point Ⓓ. **(b)** 64QAM constellation signal-to-noise ratio (CSNR) vs. symbol rate for back-to-back transmission (orange dots, b2b) and after 87km SMF (green squares). The purple curve shows the b2b CSNR for QPSK signals generated by a cutting-edge electric arbitrary-waveform generator (EAWG, Keysight M8199B). **(c) Top:** Optical spectrum of the coherently combined 288 GHz-wide spread-spectrum signal at Point Ⓓ. **Bottom:** Signal spectra with SNR of –17, –10 and –3 dB. **(d)** Measured bit error ratio (BER) of various de-spread 2 GBd QAM signals as a function of spread-spectrum SNR after transmission over 87 km SMF. The horizontal dashed lines indicate the thresholds for soft-decision forward error correction (FEC) with 7% and 20% overhead.

Hz, the phase noise of the injection-locked comb follows that of the modulation signal. Moreover, the long-term frequency stability of the comb FSR before (blue) and after (orange) injection locking and of the modulation RF signal (yellow) are measured, see Fig. 1(g). We find excellent long-term stability for RF injection locking.

Demo 1: 288 GBd 64QAM transmission

To demonstrate the performance of our OAWG system, we generate 64QAM signals with symbol rates between 160 GBd and 288 GBd by stitching four tributary signals, see top of Fig. 2(a) for the color-coded spectra of individually modulated carriers at frequencies $f_1 \dots f_4$ shown in Fig. 1(d). The bottom of Fig. 2(a) shows the spectrum of the resulting 288 GBd 64QAM. We first analyze the signal quality in back-to-back (b2b) configuration, where Point Ⓓ in Fig. 1(a) is directly connected to Point Ⓔ. To show the robustness of our system, we captured 50 waveforms for each symbol rate. The orange curve in Fig. 2(b) shows the averaged CSNR and the associated error bars of all measurements for various symbol rates up to 288 GBd. We find that the CSNR is consistently larger than 18.2 dB. To the best of our knowledge, this is the highest symbol rate so far demonstrated for 64QAM signaling. We benchmark our results to CSNR levels obtained with state-of-the-art thin-film lithium-niobate IQM with 110 GHz bandwidth, driven by a cutting-edge arbitrary waveform generator (EAWG, Keysight M8199B), purple curve in Fig. 2(b). We find that our OAWG/OAWM approach can achieve significant improvement in terms of symbol rate as well as signal quality, while the hardware requirements are relaxed in terms of bandwidth. We further demonstrate transmission of the generated 64QAM signals with various symbol rates over 87 km of SMF, with less than 1 dB CSNR penalty compared to the b2b case, green curve in Fig. 2(b). The inset shows an exemplary constellation diagram of a 64QAM signal at 288 GBd. The measured bit error ratio (BER) of 2.8×10^{-2} is well below the limit for SD-FEC with 20% overhead.

Demo 2: Spread-spectrum communications

In the second demonstration, we leverage our OAWG system for a spread-spectrum optical transmission experiment. We start from QPSK, 16QAM, 64QAM, and 128QAM signals at 2 GBd and spread their spectra by a factor of 144 by multiplying each symbol with a bipolar pseudo-noise (PN) code consisting of 144 chips [15]. The resulting 288 GHz-wide waveform is again generated by coherently combining four tributary signals. The optical spectrum of the spread-spectrum signal is shown in the top of Fig. 2(c). To demonstrate the ability to hide spread-spectrum signals in the noise floor, we attenuate the signal power using a variable optical attenuator (VOA) and superimpose it with spectrally flat amplified spontaneous emission (ASE) noise, see bottom of Fig. 2(c). Note that the noise power exceeds the signal power leading to negative SNR of –3 dB, –10 dB, and –17 dB, estimated in the optical domain. We first test the viability of the concept in a b2b configuration. At the receiver side, we use again a two-slice OAWM to reconstruct the broadband spread-spectrum signal, and we then apply a digital de-spreading algorithm to concentrate the signal power from the 288 GHz-wide spectrum to the original 2 GHz band. We estimate the processing gain by comparing the CSNR after de-spreading to the SNR of the spread-spectrum signal in the optical domain measured at Point Ⓓ, see Fig. 1(a). We obtain a processing gain of up to 24.1 dB in the low-SNR limit, only 0.5 dB away from the processing gain of 24.6 dB expected for single-polarization reception. In the second step, we perform a transmission experiment of 2 GBd spread-spectrum signals with various modulation formats over 87 km of SMF. In Fig. 2(d), we plot the measured BER vs. the SNR measured at Point Ⓓ. The results show that we can transmit all modulation formats up to 128QAM with negative SNR while the received BER is still below the limit of SD-FEC with 20% overhead. QPSK signals can even be transmitted at an SNR of –17 dB SNR, where the signal is essentially invisible in the spectrum. To the best of our knowledge, this is the first demonstration of OAWG-based spread-spectrum optical transmission.

Summary

We have demonstrated an advanced optical arbitrary waveform generator (OAWG) that exploits an RF injection-locked Kerr soliton comb as a multi-wavelength light source that can be synchronized with signal-generation electronics. We showcase the performance of the system by transmitting 64QAM signals at symbol rates of up to 288 GBd and by demonstrating spread-spectrum communications using a 288 GHz-wide optical band to transmit 2 GBd QPSK, 16QAM, 64QAM, and 128QAM signals with SNR down to –17 dB. To the best of our knowledge, our work is novel and groundbreaking in several respects, comprising the first demonstration of a Kerr-comb-based OAWG system, the transmission of 64QAM signals at record-high data rates, and the first demonstration of OAWG-based spread-spectrum optical transmission. We believe that the demonstration of Kerr-comb-based OAWG is an important step towards ultra-broadband waveform generation at THz bandwidths.

References

[1] N. K. Fontaine, D. J. Geisler, R. P. Scott, T. He, J. P. Heritage, and S. J. B. Yoo, "Demonstration of high-fidelity dynamic optical arbitrary waveform generation," *Optics Express*, 18(22), 22988-22995 (2010).
DOI: https://doi.org/10.1364/OE.18.022988..

[2] T. Henauer, A. Sherifaj, C. Füllner, W. Freude, S. Randel, T. Zwick, and C. Koos, "200 GBd 16QAM Signals Synthesized by an Actively Phase-Stabilized Optical Arbitrary Waveform Generator (OAWG)," *Optical Fiber Communication Conference* (OFC), Paper M2I.2 (2022).
DOI: https://doi.org/10.1364/OFC.2022.M2I.2.

[3] D. Drayss, D. Fang, A. Sherifaj, H. Peng, C. Füllner, T. Henauer, G. Lihachev, W. Freude, S. Randel, T. J. Kippenberg, T. Zwick, and C. Koos, "Optical Arbitrary Waveform Generation and Measurement (OAWG/OAWM) Enabling 320 GBd 32QAM Transmission," *Conference on Lasers and Electro-Optics* (CLEO*)*, Post-deadline Paper STh5C.8 (2023).

[4] V. Torres-Company, A. M. Weiner, "Optical frequency comb technology for ultra-broadband radio-frequency photonics," *Laser Photonics Review*, 8(3), 368–393 (2014).
DOI: https://doi.org/10.1002/lpor.201300126.

[5] P. Marin-Palomo, J. N. Kemal, M. Karpov, A. Kordts, J. Pfeifle, M. H. P. Pfeiffer, P. Trocha, S. Wolf, V. Brasch, M. H. Anderson, R. Rosenberger, K. Vijayan, W. Freude, T. J. Kippenberg and C. Koos, "Microresonator-based solitons for massively parallel coherent optical communications," *Nature* 546, 274–279 (2017).
DOI: https://doi.org/10.1038/nature22387.

[6] D. Drayss, D. Fang, C. Füllner, G. Likhachev, T. Henauer, Y. Chen, H. Peng, P. Marin-Palomo, T. Zwick, W. Freude, T. J. Kippenberg, S. Randel, and C. Koos, "Slice-Less Optical Arbitrary Waveform Measurement (OAWM) in a Bandwidth of More Than 600 GHz," *Optical Fiber Communications Conference and Exhibition* (OFC), Paper M2I.1 (2022).
DOI: https://doi.org/10.1364/OFC.2022.M2I.1.

[7] D. Fang, D. Drayss, G. Lihachev, P. Marin-Palomo, H. Peng, C. Füllner, A. Kuzmin, J. Liu, R. Wang, V. Snigirev, A. Lukashchuk, M. Zhang, P. Kharel, J. Witzens, C. Scheytt, W. Freude, S. Randel, T. J. Kippenberg and C. Koos, "320 GHz Analog-to-Digital Converter Exploiting Kerr Soliton Combs and Photonic-Electronic Spectral Stitching," *European Conference on Optical Communication* (ECOC), Post-deadline Paper Th3C1-PD2.2 (2021).
DOI: https://doi.org/10.1109/ECOC52684.2021.9606090.

[8] P. Trocha, M. Karpov, D. Ganin, M. H. P. Pfeiffer, A. Kordts, S. Wolf, J. Krockenberger, P. Marin-Palomo, C. Weimann, S. Randel, W. Freude, T. J. Kippenberg, C. Koos, "Ultrafast optical ranging using microresonator soliton frequency combs," *Science* 359, 887–891 (2018).
DOI: https://doi.org/10.1126/science.aao3924.

[9] D. Fang, A. Zazzi, J. Mueller, D. Drayss, C. Füllner, P. Marin-Palomo, A. T. Mashayekh, A. D. Das, M. Weizel, S. Gudyriev, W. Freude, S. Randel, J. C. Scheytt, J. Witzens, and C. Koos, "Optical Arbitrary Waveform Measurement Using Silicon Photonic Slicing Filters," *Journal of Lightwave Technology*, 40(6), 1705–1717 (2022).
DOI: https://doi.org/10.1109/JLT.2021.3130764.

[10] J. Liu, G. Huang, R. N. Wang, J. He, A. S. Raja, T. Liu, N. J. Engelsen, T. J. Kippenberg, "High-yield, wafer-scale fabrication of ultralow-loss, dispersion-engineered silicon nitride photonic circuits," *Nat. Commun.* 12, 2236 (2021).
DOI: https://doi.org/10.1038/s41467-021-21973-z.

[11] M. Blaicher, M.R. Billah, J. Kemal, T. Hoose, P. Marin-Palomo, A. Hofmann, Y. Kutuvantavida, C. Kieninger, P.-I. Dietrich, M. Lauermann, S. Wolf, U. Troppenz, M. Moehrle, F. Merget, S. Skacel, J. Witzens, S. Randel, W. Freude, and C. Koos, "Hybrid multi-chip assembly of optical communication engines by in situ 3D nano-lithography," *Light Sci. Appl.* 9, 71 (2020).
DOI: https://doi.org/10.1038/s41377-020-0272-5.

[12] J. Liu, E. Lucas, A. S. Raja, J. He, J. Riemensberger, R. N. Wang, M. Karpov, H. Guo, R. Bouchand, T. J. Kippenberg, "Photonic microwave generation in the X- and K-band using integrated soliton microcombs", *Nat. Photonics* 14, 486–491 (2020).
DOI: https://doi.org/10.1038/s41566-020-0617-x.

[13] R. Ashok, S. Naaz, R. Kamran, and S. Gupta, "An Endless Optical Phase Delay for Harmonic-Free Phase/Frequency Shifting in Coherent-Lite DCIs and Microwave Photonics," *IEEE Journal of Quantum Electronics*, 59(2), 1-10, Art no. 8000210 (2023). DOI: https://doi.org/10.1109/JQE.2023.3240735.

[14] H. Mardoyan, S. Almonacil, F. Jorge, F. Pittalà, M. Xu, B. Krueger, F. Blache, B. Duval, L. Chen, Y. Yan, X. Ye, A. Ghazisaeidi, S. Rimpf, Y. Zhu, J. Wang, M. Goix, Z. Hu, M. Duthoit, M. Gruen, X. Cai, and J. Renaudier, "First 260-GBd Single-Carrier Coherent Transmission over 100 km Distance Based on Novel Arbitrary Waveform Generator and Thin-Film Lithium Niobate I/Q Modulator," *European Conference on Optical Communication* (ECOC), Post-deadline Paper Th3C.2 (2022).

[15] D. Torrieri, *Principles of Spread-Spectrum Communication Systems*, 5th ed. Cham, Switzerland: Springer, Inc. (2022).
DOI: https://doi.org/10.1007/978-3-030-75343-6.